ORIGINAL ARTICLE

GFAP-Positive Progenitor Cell Production is Concentrated in Specific Encephalic Regions in Young Adult Mice

Zhibao Guo[1] · Yingying Su[1] · Huifang Lou[2]

Abstract Previous genetic fate-mapping studies have indicated that embryonic glial fibrillary acidic protein-positive (GFAP$^+$) cells are multifunctional progenitor/ neural stem cells that can produce astrocytes as well as neurons and oligodendrocytes throughout the adult mouse central nervous system (CNS). However, emerging evidence from recent studies indicates that GFAP$^+$ cells adopt different cell fates and generate different cell types in different regions. Moreover, the fate of GFAP$^+$ cells in the young adult mouse CNS is not well understood. In the present study, hGFAP-Cre/R26R transgenic mice were used to investigate the lineage of embryonic GFAP$^+$ cells in the young adult mouse CNS. At postnatal day 21, we found that GFAP$^+$ cells mainly generated NeuN$^+$ neurons in the cerebral cortex (both ventral and dorsal), hippocampus, and cerebellum. Strangely, these cells were negative for the Purkinje cell marker calbindin in the cerebellum and the neuronal marker NeuN in the thalamus. Thus, contrary to previous studies, our genetic fate-mapping revealed that the cell fate of embryonic GFAP$^+$ cells at the young adult stage is significantly different from that at the adult stage.

Keywords GFAP · Cell fate · Neural stem cells · Neurons · Astrocytes

✉ Zhibao Guo
zbguo130515@hotmail.com

1 Department of Neurology, Xuanwu Hospital, Capital Medical University, Beijing 100053, China

2 Zhejiang University School of Medicine, Hangzhou 310058, China

Introduction

Embryonic radial glial cells (RGCs) are bipolar cells with radial processes spanning the entire cortical wall, from the ventricular zone to the pial surface. RGCs express glial fibrillary acidic protein (GFAP) [1–4] and other astroglial markers, such as glutamate-aspartate transporter, vimentin, and RC1/2 intermediate filament epitopes [5, 6]. The earliest-established and well-documented function of RGCs is guiding neuronal migration [7]. By virtue of the radial architectural framework, newborn neurons migrate from germinal zones to their target destinations [8]. Emerging evidence from *in vivo* genetic fate-mapping studies indicates that embryonic RGCs are also multifunctional progenitor/neural stem cells and can produce astrocytes as well as neurons and oligodendrocytes throughout the adult CNS [3, 4]. However, a recent experiment demonstrated that the mouse cerebral cortex contains RGC sub-lineages with distinct fate potentials, and an RGC lineage is intrinsically specified to produce only upper-layer neurons [9]. Moreover, several studies have shown that GFAP$^+$ cells undergo dramatically divergent fates in different encephalic regions of the developing CNS. For example, early postnatal GFAP$^+$ cells give rise to astrocytes, neurons, and oligodendrocyte precursor cells in the adult cerebrum but only generate astrocytes in the adult cerebellum [10]. Similar results were found in another Cre/ loxP fate mapping study, showing that in the olfactory bulb and hippocampus, GFAP$^+$ cells mainly produce neurons as well as astrocytes and oligodendrocytes. Conversely, in the white matter and cerebral cortex, most of the GFAP$^+$ cells generate astrocytes and oligodendrocytes [11]. Since much of the existing evidence was obtained using different experimental approaches, in different encephalic regions, and across different species, there is not enough evidence

770

Neurosci. Bull. October, 2018, 34(5):769–778

to assert that all RGCs give rise to neurons in all regions of the adult CNS. In addition, the fate of GFAP$^+$ progenitor cells in the young adult mouse CNS remains unclear.

Therefore, in the present study, we set out to investigate the lineage of embryonic GFAP$^+$ cells in the young adult mouse CNS, using the human *GFAP (hGFAP)* gene promoter to drive the Cre recombinase expression in transgenic mice. We found that GFAP$^+$ cells adopt different cell fates and generate different cells types in different regions, conforming to the needs of the different neural compartments they occupy.

Materials and Methods

Transgenic Mice

The hGFAP-Cre transgenic mice were generated by Casper and McCarthy [4], and were kindly provided by Professor Shumin Duan from Zhejiang University School of Medicine, Hangzhou, China. R26R transgenic mice were purchased from Jackson Laboratory (Bar Harbor, ME). All experimental procedures were performed in accordance with protocols approved by the Institutional Animal Care and Use Committee of Xuanwu Hospital, Beijing, China.

X-Gal Staining and Immunohistochemistry

Mice were anesthetized with pentobarbital sodium (60 mg/kg, i.p.) [12], and then perfused with ice-cold phosphate-buffered saline (PBS) followed by 4% paraformaldehyde/0.1 mol/L PBS, and brains were postfixed for 2 h at 4 °C. The processing for immunohistochemistry was as described in our previous study [10].

For β-galactosidase (β-gal) histochemistry, sections were incubated in X-gal solution (5-bromo-4-chloro-3-indolyl-β-galactoside) as described previously [4, 10, 11]. Primary antibodies were applied as follows: rabbit anti-BLBP (1:1000, Chemicon, Billerica, MA), mouse anti-NeuN (1:200, Chemicon, California, USA), and rabbit anti-calbindin-D-28K (1:3000, Sigma, St. Louis, MO). Horse-radish peroxidase-conjugated secondary antibodies were from Shanghai Bohua Biotechnology Co., Ltd., Shanghai, China and diluted at 1:5000 for use. A DAB Elite kit (Beijing Zhongshan Biotechnology Co., Ltd., Beijing, China) was used to detect immunoperoxidase as directed.

Cell Counting and Microscopic Analysis

For cell counting, five sections from each brain (3 mice for each time point) were examined. Unbiased estimation was made using a computer coupled with a light microscope (DP72, Olympus, Tokyo, Japan) and Stereo Investigator

software (MicroBrightField, Colchester, VT). A sampling grid randomly placed by the software was applied to the cortex of the cerebrum and cerebellum (500×500 μm^2) and the hippocampus and thalamus (300×300 μm^2). Counting frames (300×300 μm^2 in cortex, 100×100 μm^2 in hippocampus and thalamus) were placed in the upper portion of the section as described [11]. All counting data are expressed as mean ± SD.

Results

Expression of Cre-Mediated Recombination in the Developing CNS

X-gal staining was used to identify the Cre recombinase-expressing cells. The density of X-gal$^+$ cells varied markedly among different encephalic regions in the cerebrum and cerebellum.

Expression of Cre-Mediated Recombination in the Developing Cerebrum

In the cerebrum, X-gal staining was performed on embryonic day 17.5 (E17.5) and postnatal day 21 (P21). On E17.5, nearly all X-gal$^+$ cells were distributed in the dorsal telencephalon, including the lateral cortex, medial cortex, and ganglionic eminence (Fig. 1A). However, few X-gal$^+$ cells were visible in other regions at this stage. On P21, the X-gal$^+$ cells were ubiquitously distributed throughout the gray matter and white matter of the cerebrum. A large number of X-gal$^+$ cells were seen in the dorsal and ventral cortex (Fig. 1Ba, d). The X-gal$^+$ staining was particularly striking in the pyramidal cell layer of the hippocampus and the dentate gyrus (DG) granule cell layer (Fig. 1Bb). In addition, sporadic X-gal$^+$ cells were visible in the thalamus (Fig. 1Bc).

Expression of Cre-Mediated Recombination in the Developing Cerebellum

In the cerebellum, X-gal staining was performed at several developmental stages (E12.5, E13.5, E14.5, E16.5, and P21). On E12.5, there were no X-gal$^+$ cells in the cerebellum (Fig. 2A). On E13.5, X-gal$^+$ cells were detected only in the rhombic lip (RL) (Fig. 2B). At E14.5, the X-gal$^+$ region extended from the RL to the cerebellar external granular layer (EGL). In addition, X-gal$^+$ cells were evident at the mid-hindbrain boundary (Fig. 2C). At E16.5, X-gal$^+$ cells were widely distributed throughout the cerebellum. Notably, their density was particularly striking in the EGL (Fig. 2D). At P21, X-gal$^+$ cells were ubiquitously distributed throughout the
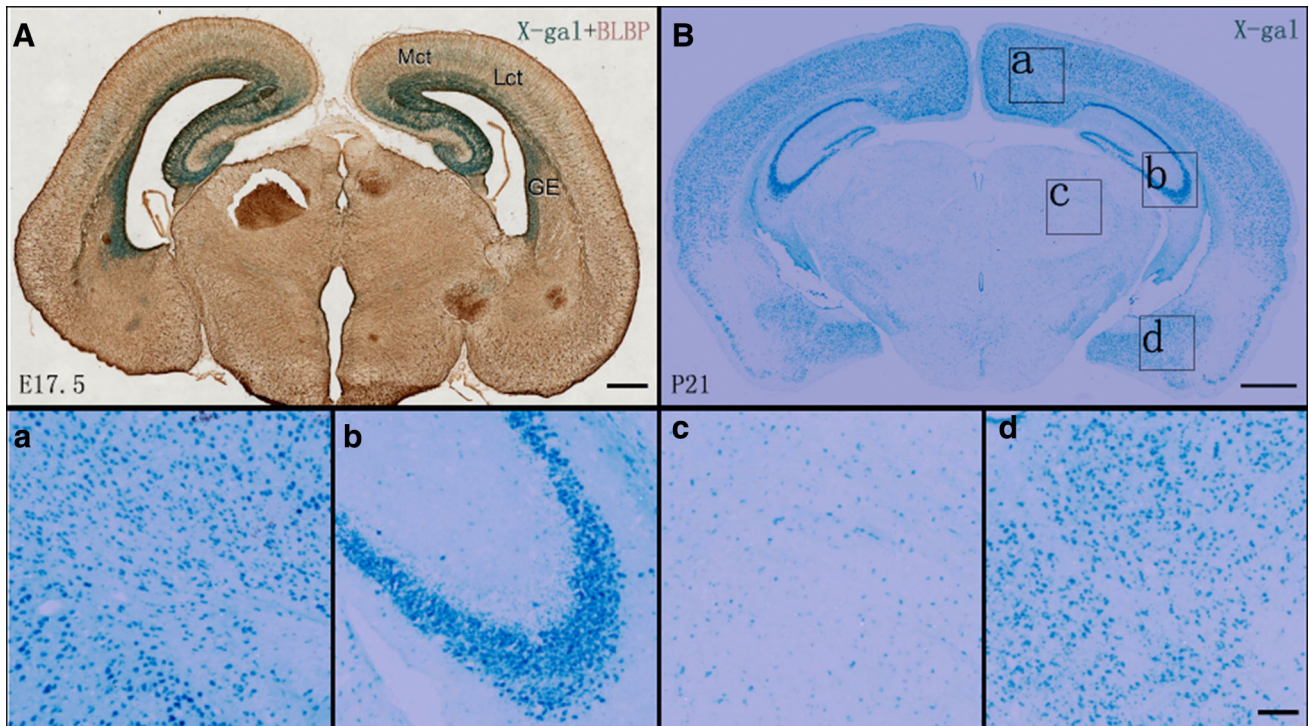
Fig. 1 Distribution of X-gal⁺ cells in the developing cerebrum of hGFAP-Cre/R26R double-transgenic mice. **A** Distribution of X-gal⁺ cells in the cerebrum at E17.5. The vast majority of X-gal⁺ cells were in the Lct, Mct, and GE. **B** Distribution of X-gal⁺ cells in the cerebrum at P21. Most of the X-gal⁺ cells were in the dorsal and ventral cortex and hippocampus. **a–d** Selected regions showing the density of X-gal⁺ cells. Lct, lateral cortex; Mct, medial cortex; GE, ganglionic eminence. Scale bars, 100 μm in **A**; 800 μm in **B**; 100 μm in **a–d**.
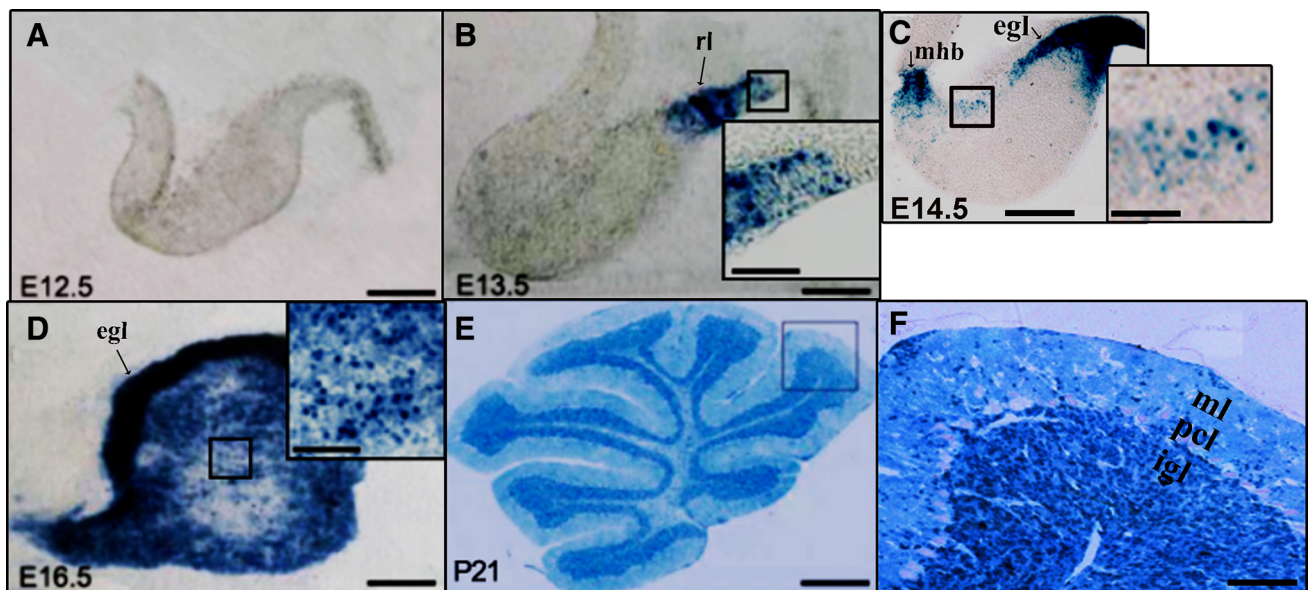

Fig. 2 Distribution of X-gal⁺ cells in the developing cerebellum of hGFAP-Cre/R26R double-transgenic mice. **A** X-gal staining showed the absence of X-gal⁺ cells at E12.5. **B** At E13.5, X-gal staining was seen in the rhombic lip (RL). **C** X-gal staining at E14.5. The RL and external granular layer (EGL) showed intense X-gal labeling, which also appeared at the mid-hindbrain boundary. **D** At E16.5, intense Cre activity was seen in the EGL. **E, F** X-gal staining at P21. mhb, mid-hindbrain boundary; ml, molecular layer; pcl, Purkinje cell layer; igl, internal granular layer. Scale bars, 100 μm in **A–D**; 25 μm in insets in **B–D**; 800 μm in **E**, and 150 μm in **F**.

cerebellum, and most were located in the internal granular layer (IGL) (Fig. 2E, F). In the molecular layer (ML), Purkinje cell layer, and medulla, only a few X-gal$^+$ cells were visible (Fig. 2E).

Identification of X-gal$^+$ Cells in the Young Adult Mouse CNS

To investigate the fates of embryonic GFAP$^+$ cells in the young adult mouse CNS, immunolabeling with cell type-specific antibodies was performed to identify the phenotypes of GFAP$^+$ cells in hGFAP-Cre/R26R double-transgenic mice at P21.

Identification of X-gal$^+$ Cells in the Young Adult Mouse Cerebrum

To determine the differentiation potential of embryonic GFAP$^+$ cells in the cortex (including the dorsal and ventral forebrain) of young adult mice, double immunolabeling with cell type-specific antibodies was performed in the superficial and deep cortex of the young adult mouse

cerebrum. The results showed that most X-gal$^+$ cells were stained with the mature neuronal marker NeuN (Fig. 3B, D), and only a few were positive for the astrocytic marker Blbp (Fig. 3A, C) in both the superficial and deep cortex. Notably, nearly all the NeuN$^+$ neurons, which were more prevalent in the deep cortex, were immunoreactive for X-gal (Fig. 3D). In contrast, only some BLBP$^+$ astrocytes were double-labeled with X-gal (Fig. 3A, C).

We used stereology [13] to evaluate the prevalence of X-gal$^+$ astrocytes and neurons derived from embryonic GFAP$^+$ cells in the ventral and dorsal cortex of the forebrain, using BLBP and NeuN as markers. Both X-gal$^+$/BLBP$^+$ astrocytes and X-gal$^+$/NeuN$^+$ neurons had similar prevalence in the ventral and dorsal cortex [dorsal 80.4% ± 1.3% and ventral 77.0% ± 2.0% X-gal$^+$ cells of neuronal lineage; dorsal 12.0% ± 3.7% and ventral 10.7% ± 3.1% X-gal$^+$ cells of astroglial lineage (Table 1)]. On the other hand, 82.3% and 85.1% of the total NeuN$^+$ neurons expressed X-gal in the ventral and dorsal cortex (Table 2), while 57.7% and 60.6% of the total BLBP$^+$ astrocytes expressed X-gal in the ventral and dorsal cortex, respectively (Table 2). These findings
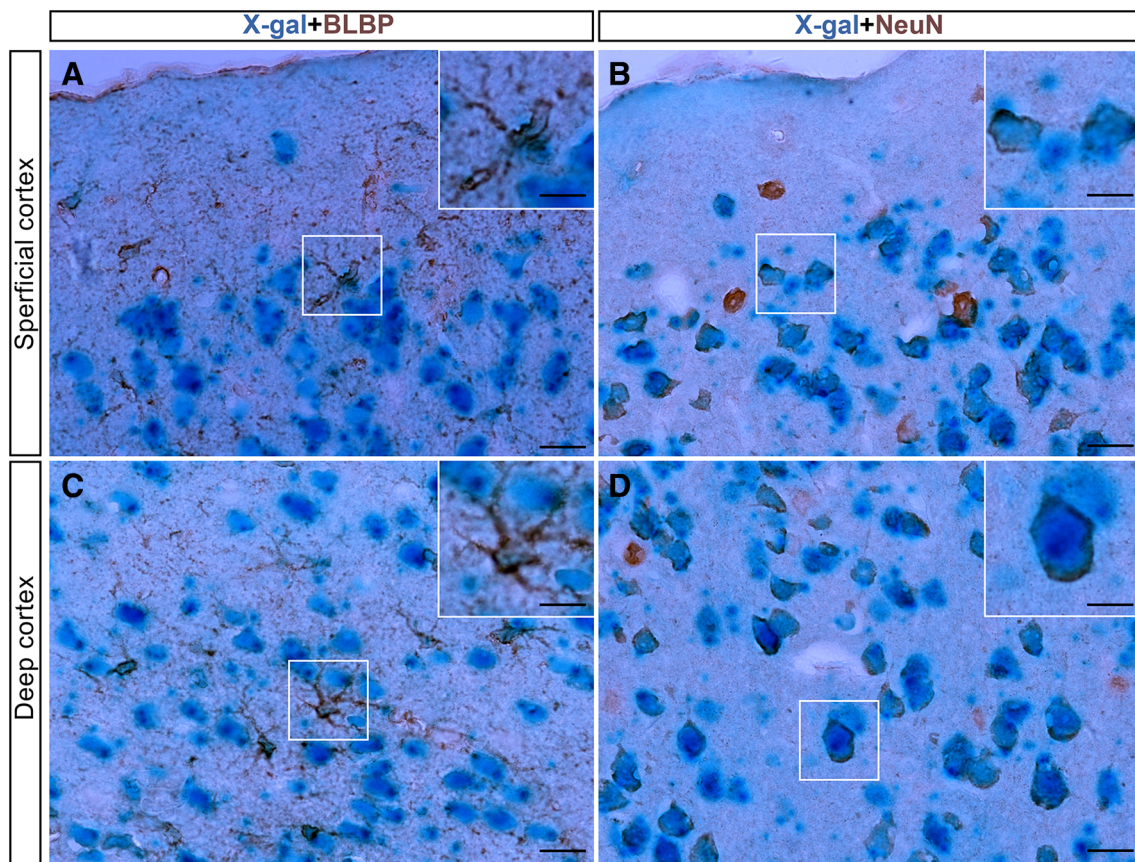

Fig. 3 Embryonic GFAP$^+$ cells mainly produce neurons in the cortex of the young adult mouse. X-gal$^+$ cells were identified using double immunohistochemical staining with antibodies for BLBP (**A**, **C**) and NeuN (**B**, **D**). Most X-gal$^+$ cells co-expressed NeuN (**B**, **D**), and only a few were stained with BLBP (**A**, **C**) in both the superficial and deep cortex of the dorsal forebrain. Scale bars, 10 μm in **A–D**; 5 μm in insets.

Table 1 Percentages of X-gal$^+$ cells expressing indicated markers in different regions at P21.

Brain region	Antibodies	
	BLBP (% ± SD)	NeuN (% ± SD)
Cerebrum		
Dorsal cortex	12.0 ± 3.7	80.4 ± 1.5
Ventral cortex	10.7 ± 3.1	77.0 ± 2.0
Hippocampus	9.1 ± 2.3	87.1 ± 4.4
Thalamus	23.3 ± 5.2	0
Cerebellum		
Molecular layer	50.1 ± 5.6	44.5 ± 6.1
Internal granular layer	ND	85.0 ± 1.3

ND not determined.

indicate that embryonic GFAP$^+$ cells are multipotent and primarily produce neurons in the cortex of the young adult mouse. At the same time, these results also suggest that embryonic GFAP$^+$ cells are not the only source of cortical astrocytes at the young adult stage.

In the hippocampus, X-gal$^+$ cells were principally located in the pyramidal cell layer (Fig. 4A, B) and the DG granule cell layer (data not shown). Immunohistochemical staining showed that the majority of the X-gal$^+$ cells were stained with the neuronal marker NeuN (Fig. 4B), and a very small proportion were positive for the astrocytic marker BLBP (Fig. 4A). Statistical analysis of cell counts showed that 87.1% ± 4.4% of X-gal$^+$ cells were of the neuronal lineage (X-gal$^+$/NeuN$^+$ neurons), and only 9.1% ± 2.3% of X-gal$^+$ cells were of the astroglial lineage (X-gal$^+$/BLBP$^+$ astrocytes) (Table 1). However, 91.8% of total NeuN$^+$ neurons and 86.4% of total BLBP$^+$ astrocytes co-expressed X-gal (Table 2). These findings suggest that embryonic GFAP$^+$ cells mainly give rise to neurons, rather than astrocytes, in the hippocampus of the

young adult mouse. In addition, embryonic GFAP$^+$ cells are the main source of neurons at the young adult stage.

In the thalamus, there were some sporadic X-gal$^+$ cells with oval-shaped somata and slender processes. Immunohistochemical staining showed that a small proportion of the X-gal$^+$ cells co-expressed BLBP (Fig. 4C). Surprisingly, all the X-gal$^+$ cells were negative for NeuN (Fig. 4D). Estimation of the prevalence of X-gal$^+$ astrocytes in this region showed that 23.3% ± 5.2% of X-gal$^+$ cells were BLBP$^+$ astrocytes (Table 1) and 41.7% of total BLBP$^+$ astrocytes co-expressed X-gal (Table 2). These observations indicate that embryonic GFAP$^+$ cells are the main source of astrocytes, but not of neurons, in the thalamus at the young adult stage.

Identification of X-gal$^+$ Cells in the Young Adult Mouse Cerebellum

To identify the type(s) of X-gal$^+$ cells in the cerebellum at P21, BLBP, NeuN, and calbindin were used to label astrocytes (including Bergmann glia), granule cells, and Purkinje cells, respectively [14]. Immunostaining showed that most of the X-gal$^+$ cells co-expressed NeuN in the IGL (Fig. 5D), and a number of X-gal$^+$ cells were stained with BLBP (Fig. 5A) and NeuN (Fig. 5C) in the ML. However, there were no X-gal$^+$ cells immune-positive for calbindin (Fig. 5B). Cell counts showed that 85.0% ± 1.3% and 44.5% ± 6.1% of X-gal$^+$ cells were NeuN$^+$ neurons in the IGL and ML, respectively (Table 1). Meanwhile, 58.8% and 50.2% of total NeuN$^+$ neurons co-expressed X-gal in the IGL and ML, respectively (Table 2). On the other hand, in the ML, 50.1% ± 5.6% of X-gal$^+$ cells were BLBP$^+$ astrocytes (Table 1), and 76.7% of total BLBP$^+$ astrocytes co-expressed X-gal (Table 2). In addition, we counted more than 300 calbindin$^+$ Purkinje cells, but none were positive for X-gal (Table 2). These findings indicated that embryonic GFAP$^+$ cells mainly generate NeuN$^+$ neurons

Table 2 Cell populations derived from GFAP-positive progenitors.

| Brain region	Percentage of β-gal$^+$ neurons (*n* = # NeuN$^+$ cells)	Percentage of β-gal$^+$ astrocytes (*n* = # BLBP$^+$ cells)	Percentage of β-gal$^+$ Purkinje cells (*n* = # calbindin$^+$ cells)
Cerebrum			
Dorsal cortex	85.1% (*n* = 809)	60.6% (*n* = 197)	ND
Ventral cortex	82.3% (*n* = 507)	57.7% (*n* = 205)	ND
Hippocampus	91.8% (*n* = 1000)	86.4% (*n* = 150)	ND
Thalamus	0 (*n* = 397)	41.7% (*n* = 177)	ND
Cerebellum			ND
Molecular layer	50.2% (*n* = 97)	76.7% (*n* = 212)	ND
Purkinje cell layer	ND	ND	0 (*n* = 355)
Internal granular layer	58.8% (*n* = 980)	ND	ND

ND not determined.
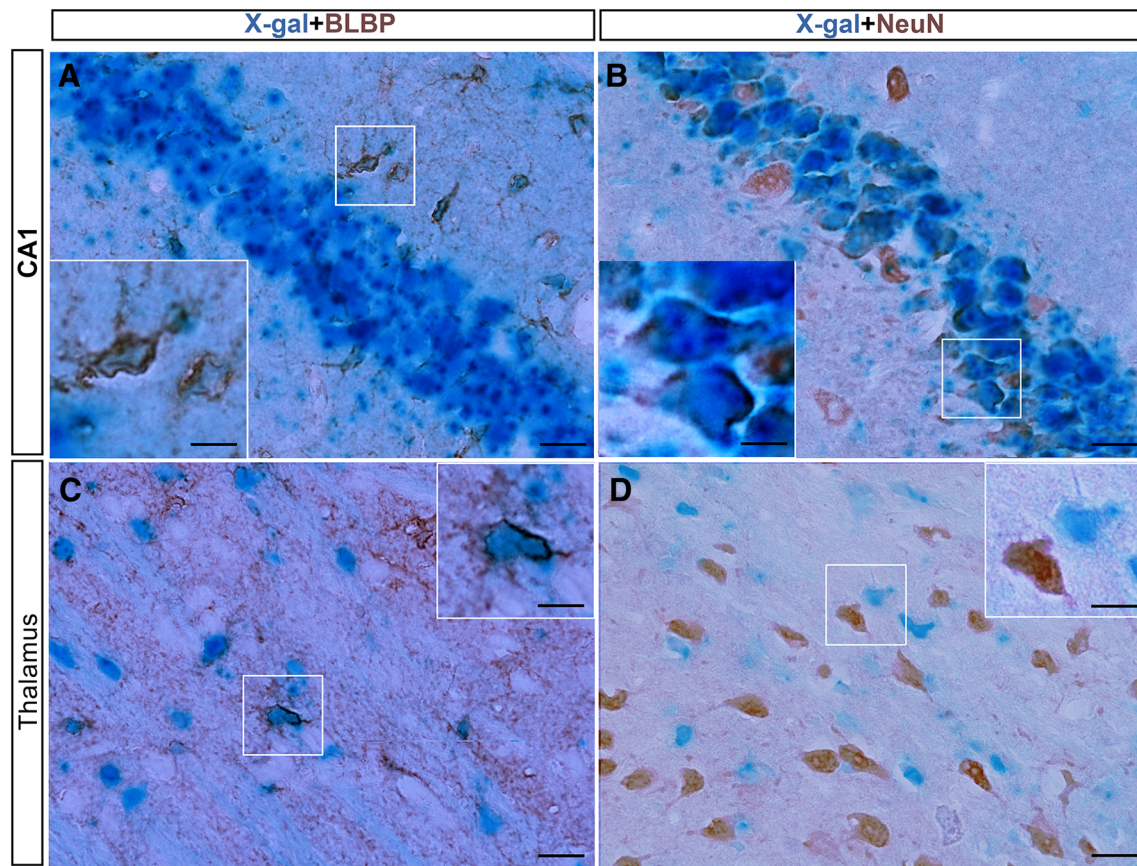
Fig. 4 Embryonic GFAP$^+$ cells mainly produce hippocampal neurons and thalamic astrocytes in young adult mice. **A** A few X-gal$^+$ cells co-expressed BLBP in CA1 of the hippocampus. **B** Nearly all the X-gal$^+$ cells were positive for NeuN in CA1 of the hippocampus. **C** A small proportion of X-gal$^+$ cells were positive for BLBP in the thalamus. **D** All the X-gal$^+$ cells were negative for NeuN in the thalamus. Scale bars; 10 μm in **A–D**; 4 μm (insets in **A**, **B**); 5 μm (insets in **C**, **D**).

and BLBP$^+$ astrocytes, but do not produce Purkinje cells in the young adult cerebellum.

Discussion

In the present study, we used hGFAP-Cre/R26R double transgenic mice to tag embryonic GFAP$^+$ cells and trace their lineage in the young adult mouse CNS. Genetic fate-mapping demonstrated that the GFAP$^+$ progenitor cells mainly produced neurons, rather than astrocytes, in the cerebral cortex (both ventral and dorsal), hippocampus, and cerebellar IGL at the young adult stage. In addition, GFAP$^+$ cells did not generate thalamic neurons or cerebellar Purkinje cells.

Region-Specific Differences in hGFAP-Cre-Mediated Recombination in the Young Adult Mouse CNS

We monitored the expression of Cre recombinase driven by the hGFAP promoter using X-gal staining at several time points. We found that the spatial and temporal patterning of Cre recombinase varied markedly among different encephalic regions in the cerebrum and cerebellum. For example, the onset of Cre expression began in the cerebellar RL by E13.5, suggesting that the hGFAP promoter is active in multi-potent neural stem cells (Fig. 2B) [15]. Furthermore, X-gal$^+$ cells were non-homogenously distributed in different regions of the cerebrum and cerebellum in the young adult mouse CNS. In the cerebrum at P21, the X-gal$^+$ staining was particularly striking in the pyramidal cell layer of the hippocampus and the granule cell layer of the DG (Fig. 1Bb). However, only sporadic X-gal$^+$ cells were visible in the thalamus (Fig. 1Bc). In the cerebellum, a large proportion of X-gal$^+$ cells were located in the IGL and only a few were visible in the ML, Purkinje cell layer, and medulla (Fig. 2E, F). These observations indicated that the progeny of GFAP$^+$ progenitor cells differ profoundly between different brain regions [2]. Compared with data from several previous reports, we have provided a more
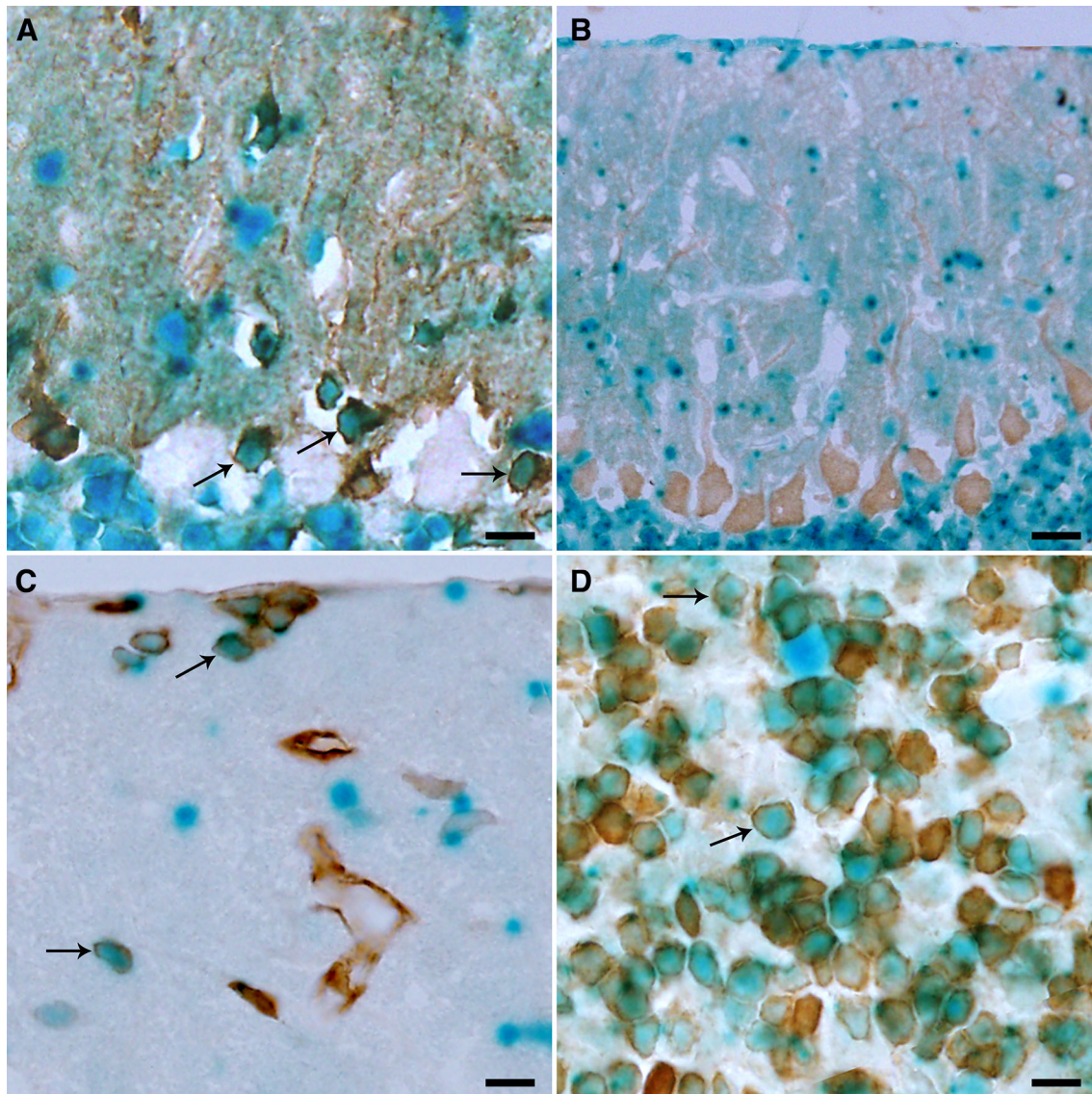
Fig. 5 Embryonic GFAP⁺ cells produce neurons and astrocytes, but not Purkinje cells, in the young adult mouse cerebellum. **A** A large proportion of X-gal⁺ cells in the ML co-expressed BLBP. **B** All the X-gal⁺ cells were negative for calbindin. **C** A small proportion of X-gal⁺ cells in the ML were immune-positive for NeuN. **D** Most of the X-gal⁺ cells in the IGL were positive for NeuN. Arrows indicate examples of X-gal⁺/marker⁺ cells. Scale bars, 11.3 μm in **A**; 22.5 μm in **B**; and 7.5 μm in **C** and **D**. IGL, internal granular layer; ML, molecular layer.

comprehensive and detailed characterization of the pattern of Cre expression [2, 4, 16].

Neurogenic Potential of GFAP⁺ Progenitor Cells in the Young Adult Thalamus

Two early *in vivo* fate mapping studies using the same hGFAP promoter fragment to drive Cre recombinase expression have reported different results [2, 4]. One experiment found that GFAP-expressing progenitor cells produced neurons throughout the CNS, and there was very little regional heterogeneity in the neurogenic potential of

RGCs between the ventral and dorsal telencephalon. Moreover, much higher reporter gene expression was detected in thalamic neurons – 40% of total NeuN⁺ neurons, 34% of total calbindin⁺ neurons, and 43% of total calretinin⁺ neurons expressed X-gal [4]. However, experimental data from the other study suggested that the neurogenic potential of GFAP-expressing precursors is fundamentally different in the ventral and dorsal telencephalon. While GFAP⁺ cells generated a large number of neurons in the dorsal telencephalon, few neurons were produced from radial glia in the ventral telencephalon. In addition, the findings indicated that GFAP⁺ cells gave rise

776

Neurosci. Bull. October, 2018, 34(5):769–778

to the vast majority of cortical projection neurons but few interneurons [2]. A recent experiment also demonstrated that GFAP$^+$ cells vary dramatically in their ability to generate divergent populations of neurons in different encephalic regions of the developing CNS [9]. In our previous study, hGFAP-Cre-ER^{T2} transgenic mice and R26R mice were used to investigate the cell fate of early postnatal GFAP-positive cells. Our genetic fate-mapping showed that the reporter gene is highly expressed in the thalamus, and GFAP$^+$ cells mainly generate astrocytes as well as a few NG2 glia but not NeuN-positive neurons [10]. In the present study, we found that 23.3% of X-gal$^+$ cells in the thalamus were BLBP$^+$ astrocytes. However, no X-gal$^+$/NeuN$^+$ neurons were detected in this region (Figs. 4D, 6; Tables 1, 2). It is clear that GFAP-expressing progenitor cells do not generate thalamic neurons at the young adult stage. Therefore, it is possible that another source of thalamic neurons exists at this stage. For example, *in vivo* cell fate-mapping studies have demonstrated that NG2 glia are capable of serving as neural precursors and generate some neurons in the hypothalamus of the adult brain [17, 18]. However, the role of NG2 glia in neurogenesis in the mouse thalamus is still not fully elaborated.

GFAP$^+$ Progenitor Cells Do Not Generate Purkinje Neurons in the Young Adult Cerebellum

Both a previous study and ours found that the expression of Cre recombinase driven by the hGFAP promoter can be detected at an early embryonic stage in the developing cerebellum [19]. In the young adult cerebellum (P21), X-gal$^+$ cells were ubiquitously distributed throughout the cerebellum, most located in the IGL and few in the ML and Purkinje cell layer (Fig. 2E, F). Using hGFAP-Cre/Rosa26R double transgenic mice, a previous experiment
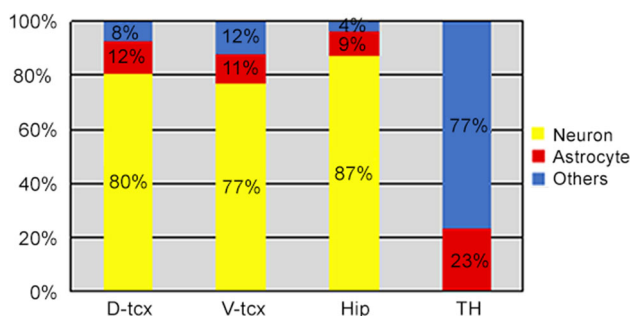

Fig. 6 Composition of progeny of embryonic GFAP$^+$ progenitors in different encephalic regions of the mouse at P21. Note that embryonic GFAP$^+$ cells mainly produce neurons, not astrocytes, in the cortex and hippocampus of the young adult mouse. However, in the thalamus, the GFAP$^+$ cells do not produce neurons. D-tcx, dorsal cortex; V-tcx, ventral cortex; Hip, hippocampus; TH, thalamus.

showed that GFAP-positive progenitors produce 39% of calbindin$^+$ Purkinje cells in the cerebellum. Interestingly, there are differences in the number of Purkinje cells that undergo recombination between the transgenic lines, and very few double-positive Purkinje neurons are detectable in the other hGFAP-Cre lines and the mGFAP-Cre lines [4]. Previous studies with hGFAP-Cre-ER^{T2}/R26R mice indicated that early postnatal GFAP$^+$ cells do not generate calbindin$^+$ Purkinje cells in the adult cerebellum [10, 11]. In the present study, to identify whether GFAP$^+$ cells produce Purkinje cells in the young adult cerebellum, calbindin was used to label Purkinje cells, and the results showed that no X-gal$^+$ cells were immune-positive for calbindin (Fig. 5B; Table 2). The failure to detect reporter-positive Purkinje neurons in the young adult brain may be due to the fact that the precursor cells for Purkinje cells do not express the GFAP promoter; this could also be because these progenitors differentiate prior to GFAP promoter activation [4].

Astrocytic Fate of GFAP$^+$ Progenitor Cells in the Young Adult Hippocampus

Astrocytes, the most abundant cell type in the CNS [20, 21], are first detectable at a late gestational stage ($\sim$ E16) and are predominantly produced during the first three weeks after birth [22, 23]. Based on their unique morphology, astrocytes can roughly be divided into protoplasmic astrocytes in the gray matter and fibrous astrocytes in the white matter [23]. It is well known that astrocytes play a series of crucial roles in structural support, ion homeostasis, blood–brain barrier function, synaptic plasticity, and repair following traumatic injury [24, 25]. Astrocytes are reportedly generated from two sources: radial glia in the ventricular zone and progenitor cells in the subventricular zone [26–28]. Recently, it has been reported that progenitors from the ventral hippocampus contribute to the neural stem cells in the DG subgranular zone, and these cells have an ability to self-renew and generate new astrocytes in the hippocampus [29]. In addition, several *in vivo* genetic fate-mapping studies have indicated that embryonic NG2 cells generate protoplasmic astrocytes in the hippocampus [30–32]. This implies that NG2 glia may be another source of hippocampal astrocytes.

As is well known, astrocytes are abundant in the hippocampus. In our study, we found that a vast number of X-gal$^+$ cells were distributed in the pyramidal cell layer of the hippocampus and the granule cell layer of the DG. Unexpectedly, immunostaining and cell-counts showed that only a small proportion (9.1%) of X-gal$^+$ cells were BLBP$^+$ astrocytes (Figs. 4B, 6; Table 1). A previous study that used the same hGFAP-Cre/R26R mice also failed to

observe recombination in a majority of GFAP-expressing astrocytes in the adult hippocampus [4]. Together, these findings suggest that either the Cre reporter line, R26R, is inefficient at detecting Cre-mediated recombination in astrocytes, or the Cre recombinase expressed in astrocytes is non-functional [4].

Overall, in contrast to previous studies, our findings demonstrate that the cell fate of embryonic GFAP$^+$ cells at the young adult stage is markedly different from that at the adult stage. Moreover, the region-specific difference in the lineage of RGCs from different encephalic regions emphasizes the importance of not generalizing the lineage of RGCs across species or CNS regions. Understanding the signaling mechanisms that contribute to the development of RGCs and their generation of diverse populations of cell types in the CNS may provide new therapeutic avenues for relevant neurological diseases. Finally, a significant question raised by our study is whether the region-specific differences in the progeny of GFAP$^+$ progenitors is due to the intrinsic characteristics of RGCs, or whether they are influenced by the local environment. Future experiments will further explore these events.

Compliance with Ethical Standards

Conflict of interest All authors claim that there are no conflicts of interest.

References

1. Malatesta P, Harfuss E, Gotz M. Isolation of radial glial cells by fluorescent-activated cell sorting reveals a neuronal lineage. Development 2000, 127: 5253–5263.
2. Malatesta P, Hack MA, Hartfuss E, Kettenmann H, Klinkert W, Kirchnoff F, et al. Neuronal or glial progeny: regional differences in radial glia fate. Neuron 2003, 37: 751–776.
3. Anthony TE, Klein C, Fishell G, Heintz N. Radial glia serve as neuronal progenitors in all regions of the central nervous system. Neuron 2004, 41: 881–890.
4. Casper KB, McCarthy KD. GFAP-positive progenitor cells produce neurons and oligodendrocytes throughout the CNS. Mol Cell Neurosci 2006, 31: 676–684.
5. Misson JP, Edwards MA, Yamamoto M, Caviness Jr VS. Identification of radial glial cells within the developing murine central nervous system: studies based upon a new immunohistochemical marker. Brain Res Dev Brain Res 1988, 44: 95–108.
6. Kriegstein AR, Gotz M. Radial glia diversity: a matter of cell fate. Glia 2003, 43: 37–43.
7. Rakic P. Mode of cell migration to the superficial layers of fetal monkey neocortex. J Comp Neurol 1972, 145: 61–83.
8. Xu H, Yang Y, Tang X, Zhao M, Liang F, Xu P, et al. Bergmann glia function in granule cell migration during cerebellum development. Mol Neurobiol 2013, 47: 833–844.
9. Franco SJ, Gil-Sanz C, Martinez-Garay I, Espinosa A, Harkins-Perry SR, Ramos C, et al. Fate-restricted neural progenitors in the mammalian cerebral cortex. Science 2012, 337: 746–749.
10. Guo Z, Wang X, Xiao J, Wang Y, Lu H, Teng J, et al. Early postnatal GFAP-expressing cells produce multilineage progeny in cerebrum and astrocytes in cerebellum of adult mice. Brain Res 2013, 532: 14–20.
11. Ganat YM, Silbereis J, Cave C, Ngu H, Anderson GM, Ohkubo Y, et al. Early postnatal astroglial cells produce multilineage precursors and neural stem cells in vivo. J Neurosci 2006, 26: 8609–8621.
12. Zhang T, Tanida M, Uchida K, Suzuki Y, Yang W, Kuda Y, et al. Mouse anaphylactic hypotension is characterized by initial baroreflex independent renal sympathoinhibition followed by sustained renal sympathoexcitation. Front Physiol 2017, 8: 669.
13. Guo F, Ma J, McCauley E, Bannerman P, Pleasure D. Early postnatal proteolipid promoter-expressing progenitors produce multilineage cells in vivo. J Neurosci 2009, 29: 7256–7270.
14. Sudarov A, Joyner AL. Cerebellum morphogenesis: the foliation pattern is orchestrated by multi-cellular anchoring centers. Neural Dev 2007, 2: 26.
15. Zhuo L, Theis M, Alvarez-Maya I, Brenner M, Willecke K, Messing A. hGFAP-cre transgenic mice for manipulation of glial and neuronal function in vivo. Genesis 2001, 31: 85–94.
16. Wen J, Yang HB, Zhou B, Lou HF, Duan S. β-Catenin is critical for cerebellar foliation and lamination. PLoS One 2013, 8: e64451.
17. Rivers LE, Young KM, Rizzi M, Jamen F, Psachoulia K, Wade A, et al. PDGFRA/NG2 glia generate myelinating oligodendrocytes and piriform projection neurons in adult mice. Nat Neurosci 2008, 11: 1392–1401.
18. Robins SC, Trudel E, Rotondi O, Liu X, Djogo T, Kryzskaya D, et al. Evidence for NG2-glia derived, adult-born functional neurons in the hypothalamus. PLoS One 2013, 8: e78236.
19. Bajenaru ML, Zhu Y, Hedrick NM, Donahoe J, Parada LF, Gutmann DH. Astrocyte-specific inactivation of the neurofibromatosis 1 gene (NF1) is insufficient for astrocytoma formation. Mol Cell Biol 2002, 22: 5100–5113.
20. Clarke LE, Barres BA. Emerging roles of astrocytes in neural circuit development. Nat Rev Neurosci 2013, 14: 311–321.
21. Namihira M, Nakashima K. Mechanisms of astrocytogenesis in the mammalian brain. Curr Opin Neurobiol. 2013, 23: 921–927.
22. Ge WP, Miyawaki A, Gage FH, Jan YN, Jan LY. Local generation of glia is a major astrocyte source in postnatal cortex. Nature 2012, 484: 376–380.
23. Bayraktar OA, Fuentealba LC, Alvarez-Buylla A, Rowitch DH. Astrocyte development and heterogeneity. Cold Spring Harb Perspect Biol 2014, 7: a020362.
24. Ota Y, Zanetti AT, Hallock RM. The role of astrocytes in the regulation of synaptic plasticity and memory formation. Neural Plast 2013, 2013: 85463.
25. Guérout N, Li X, Barnabé-Heider F. Cell fate control in the developing central nervous system. Exp Cell Res 2014, 321: 77–83.
26. Cameron RS, Rakic P. Glial cell lineage in the cerebral cortex: a review and synthesis. Glia 1991, 4: 124–137.
27. Marshall CA, Suzuki SO, Goldman JE. Gliogenic and neurogenic progenitors of the subventricular zone: who are they where did they come from and where are they going? Glia 2003, 43: 52–61.
28. Kriegstein A, Alvarez-Buylla A. The glial nature of embryonic and adult neural stem cells. Annu Rev Neurosci 2009, 32: 149–184.

29. Li G, Fang L, Fernández G, Pleasure SJ. The ventral hippocampus is the embryonic origin for adult neural stem cells in the dentate gyrus. Neuron 2013, 78: 658–672.

30. Zhu X, Hill RA, Nishiyama A. NG2 cells generate oligodendrocytes and gray matter astrocytes in the spinal cord. Neuron Glia Biol 2008, 4: 19–26.

31. Zhu X, Hill RA, Dietrich D, Komitova M, Suzuki R, Nishiyama A. Age-dependent fate and lineage restriction of single NG2 cells. Development 2011, 138: 745–753.

32. Huang W, Zhao N, Bai X, Karram K, Trotter J, Goebbels S, et al. Novel NG2-CreERT2 knock-in mice demonstrate heterogeneous differentiation potential of NG2 glia during development. Glia 2014, 62: 896–913.